



## Theoretical Analysis of Grain Size Influence on Electrical Conductivity in Nickel and Copper

Sadeem Abbas Fadhil<sup>1,\*</sup>, Saif M. Jasim<sup>1</sup>, Ghasaq Talal Suhail<sup>2</sup>, Sara M Ibraheim<sup>1</sup>

<sup>1</sup> Department of Physics, College of Sciences, Al-Nahrain University, 10070, Baghdad, Iraq

<sup>2</sup> Department of Forensic Science, College of Sciences, Al-Nahrain University, 10070, Baghdad, Iraq

### Article's Information

Received: 04.04.2025  
Accepted: 29.07.2025  
Published: 15.12.2025

### Keywords:

Electrical conductivity,  
Copper,  
Nickel,  
Time of events theory,  
Modelling.

### Abstract

This work presents a new model for electrical conductivity versus grain size derived from a new theory called the time of events theory. The time of events (TE) model was applied to experimental data of electrical conductivity versus grain sizes of two metals, copper Cu and Nickel Ni due to their industrial importance in transferring electricity and electrical circuits. In addition, a comparative analysis of two other models was applied to the experimental data. The Maydas-Shatzkes model and the Andrews model. The newly derived model showed the best agreement with experimental data of Cu and Ni among all models. It uses mainly three factors: the first one is for extremely tiny grain sizes, while the second is for small grain sizes, and the third is for relatively large grain sizes. From comparing the fitting data with the Andrews models, it was noticed that the third parameter values were close to the Andrews model parameter. Therefore, Andrews' model is well applied to large grain sizes, but it deviates at extremely tiny grain sizes. This new model also predicted that the Ni data have minima and maxima, while other models did not have such a prediction.

<http://doi.org/10.22401/ANJS.28.4.09>

\*Corresponding author: [sadeemfadhil@yahoo.com](mailto:sadeemfadhil@yahoo.com)



This work is licensed under a [Creative Commons Attribution 4.0 International License](https://creativecommons.org/licenses/by/4.0/)

### 1. Introduction

Nanoscale brought many new properties that enhanced the performance in mechanical, electrical, and many other materials properties [1]–[3]. Understanding the mechanism of the electrical conductivity in metals as a function of nanometer-sized grains is crucial for many applications, including interconnect lines [4][5]. The grain size has a strong effect on electrical conductivity, as several works concluded [6][7]. Generally, decreasing grain size leads to increasing the surface area, which is associated with decreasing electrical conductivity due to increased scattering centers on grain boundaries [8]. Regardless, many other factors that are related to grains may affect the electrical conductivity of different materials, as an example, the tilt angle of grains is found to affect the electrical conductivity, as found by [8][9]. Given this complexity, several theoretical models were developed to interpret the behavior of electrical conductivity versus grain size. Most models that interpret electrical conductivity are based on

classical procedures [10][11]. However, some models tried using the quantum approach, but unfortunately faced difficulties such as the defects in thin films that usually largely affect the electrical conductivity, and it is not easy to count quantumly [12]. Therefore, the classical approaches appears dominated. These approaches started with Fuchs [13] who assumed increasing resistivity due to surface scattering mainly in thin films and interconnecting wires. Some works later have included surface roughness to count for additional scattering effects [14][15]. Maydas-Shatzkes model [16]. Assuming the scattering of electrons from grain boundaries decreasing the grain size leads to an increase in the number of scattered electrons which causes lower conductivity [17]–[19]. They also assumed a reflection coefficient related to electrons' back reflection when facing grain boundaries. Andrews [20] formulated a model that assumed the resistivity is proportional to the grain boundary surface area relative to volume, i.e., it is inversely proportional to grain size diameter. He

postulated a proportionality constant named Anderew's constant. A. Bakonyi [21] compared the Maydas-Shatzkes model and the Andrews model, and concluded that the Andrews model is more reliable and easier to apply to experimental data, due to the large scatter of the reflection factor found from different experimental data for a given metal. However, comparing the Andrews model with experimental data does not account for all the factors that affect the electrical conductivity in metals as we will see in the present work. The present work derives a new model to better fit the experimental data by bringing new factors yielded from a new multiscale models [22][23] based on a new theory called the Time of events theory [24]. This theory proved its success in interpreting many physical phenomena from atoms to galaxies by introducing a new multiscale model capable of manipulating different physical processes at different scales [25]–[28].

## 2. Theoretical Model Derivation

The current model derived from the theory of Time of events. This theory has shown excellence in interpreting the variations of different physical properties with different scales, especially the mesoscale. Equation (1) from ref. [22] gives

$$\sum_{i=1}^n \left(\frac{K_i}{m_i}\right) - \sum_{i=1}^n \sum_{\substack{j=1 \\ j \neq i}}^n \left(\frac{V_{ij}}{m_i}\right) = E_t \sum_{i=1}^n \frac{1}{m_i} \dots (1)$$

where  $K_i$ ,  $V_{ij}$ ,  $E_t$ , and  $m_i$  are the kinetic energy, potential energy from the electromagnetic interaction between the  $i$ th and the  $j$ th particles, total energy, and particle mass of the  $i$ th particle, respectively. In metals, the particles can be assumed to be composed of free electrons and the cores that contain inner electrons and the nucleus. Therefore equation (1) can be reformulated as:

$$\sum_{i=1}^{n_e} \left(\frac{K_{ie}}{m_{ie}}\right) + \sum_{i=1}^{n_c} \left(\frac{K_{ic}}{m_{ic}}\right) - \sum_{i=1}^n \sum_{\substack{j=1 \\ j \neq i}}^n \left(\frac{V_{ij}}{m_i}\right) = E_t \sum_{i=1}^n \frac{1}{m_i} \dots (2)$$

where sub symbols e and c represent the valence (free electrons) and the cores respectively. For a certain material, the cores and valence electrons should be the same throughout the whole sample, therefore we can take them out of the summation, and after multiplying by  $m_c$  it becomes:

$$\begin{aligned} \frac{m_c}{m_e} \sum_{i=1}^{n_e} K_{ie} + \sum_{i=1}^{n_c} K_{ic} - m_c \sum_{i=1}^n \sum_{\substack{j=1 \\ j \neq i}}^n \left(\frac{V_{ij}}{m_i}\right) \\ = E_t m_c \sum_{i=1}^n \frac{1}{m_i} \dots (3) \\ K_e = \frac{1}{2} m_e v_e^2 \dots (4) \end{aligned}$$

where  $v_e$  is the electron's velocity given as:

$$v_e = \mu_e E,$$

Where  $\mu_e$  and  $E$  are the electron mobility and electric field, respectively. Therefore,  $K_e$  can be written as:

$$K_e = \frac{1}{2} m_e v_e^2 = \frac{1}{2} m_e \mu_e^2 E^2 \dots (5)$$

But from Ohm's law

$$J = \sigma E = \rho_v \mu \dots (6)$$

where  $J$ ,  $\sigma$ ,  $\rho_v$ , and  $\mu$  are the current density, electrical conductivity, volume charge density, and charge mobility, respectively.  $\rho_v$  equals the electric charge  $e$  times the charge density  $n$ . Therefore;

$$\sigma = en\mu \Rightarrow \mu = \frac{\sigma}{en} \dots (7)$$

Substituting eq. (7) in eq. (5) gives:

$$K_e = \frac{1}{2} m_e \left(\frac{\sigma_e}{en_e}\right)^2 E^2 \dots (8)$$

But

$$\rho_v = en_e \dots (9)$$

So,

$$K_e = \frac{1}{2} m_e \left(\frac{\sigma_e}{\rho_v}\right)^2 E^2 \dots (10)$$

Substituting equation (10) in equation (3) gives:

$$\begin{aligned} \frac{m_c}{m_e} \sum_{i=1}^{n_e} \frac{1}{2} m_e \left(\frac{\sigma_{ei}}{\rho_{iv}}\right)^2 E^2 + \sum_{i=1}^{n_c} K_{ic} - m_c \sum_{i=1}^n \sum_{\substack{j=1 \\ j \neq i}}^n \left(\frac{V_{ij}}{m_i}\right) \\ = E_t m_c \sum_{i=1}^n \frac{1}{m_i} \dots (11) \end{aligned}$$

The term  $K_{ic}$  can be neglected, due to relatively large core masses. Rearranging the above equation and yields:

$$m_c \sum_{i=1}^{n_e} \frac{1}{2} \left(\frac{\sigma_{ei}}{\rho_{iv}}\right)^2 E^2 = E_t m_c \sum_{i=1}^n \frac{1}{m_i} + m_c \sum_{i=1}^n \sum_{\substack{j=1 \\ j \neq i}}^n \left(\frac{V_{ij}}{m_i}\right) \dots (12)$$

Dividing equation (12) by  $m_c$ , then factorizing all terms in the left-hand side of equation (12) except  $\sigma_{ei}$  yields:

$$\sum_{i=1}^n \sigma_{ie}^2 = \frac{2}{E^2} \left( \frac{E_t \sum_{i=1}^n \frac{1}{m_i} + \sum_{i=1}^n \sum_{\substack{j=1 \\ j \neq i}}^n \left(\frac{V_{ij}}{m_i}\right)}{\sum_{i=1}^n \frac{1}{\rho_{iv}}} \right) \dots (14)$$

For an isotropic material and noting that E is independent of grain size, equation (14) will be as follows:

$$\sigma_{ie}^2 \propto \left[ \frac{0.5E_t \left( \left( \frac{n}{m_e} \right) + \left( \frac{n}{m_c} \right) + \frac{n}{m_c} \sum_{j=1}^n \left( \frac{V_{ij}}{m_i} \right) + \frac{n}{m_e} \sum_{j=1}^n \left( \frac{V_{ij}}{m_i} \right) \right)}{\frac{n}{\rho_{iv}}} \right] \quad \dots (15)$$

Eliminating n from the denominator and numerator in addition to constants yields:

$$\sigma_{ie}^2 \propto \left[ \frac{E_t \left( \left( \frac{1}{m_e} \right) + \left( \frac{1}{m_c} \right) + \frac{1}{m_c} \sum_{j=1}^n \left( \frac{V_{ij}}{m_i} \right) + \frac{1}{m_e} \sum_{j=1}^n \left( \frac{V_{ij}}{m_i} \right) \right)}{\frac{1}{\rho_v}} \right] \quad \dots (16)$$

Knowing that

$$\sum_{j=1}^n V_{ij} = \sum_{j=1}^n \frac{Q_i Q_j}{r_{ij}} \Rightarrow \sum_{j=1}^n V_{ij} \propto \sum_{j=1}^n \frac{1}{r_{ij}} \quad \dots (17)$$

Also

$$\rho_v = \frac{Q}{\frac{4}{3}\pi r^3} \propto \frac{1}{r^3} \quad \dots (18)$$

And

$$m = \frac{4}{3}\rho_m \pi r^3 \propto r^3 \quad \dots (19)$$

Where  $\rho_m$  is the mass density of the material. Substituting equations (17), (18), and (19) in equation (16) yields after neglecting constants and r-independent terms:

$$\begin{aligned} \sigma_{ie}^2 &\propto \left[ \frac{\left( \left( \frac{1}{m_e} \right) + \left( \frac{1}{r^3} \right) + \frac{1}{r^4} + \frac{1}{r} \right)}{\frac{1}{r^3}} \right] \\ &= \left( \frac{r^3}{m_e} + \left( \frac{r^3}{r^3} \right) + \frac{r^3}{r^4} + \frac{r^3}{r} \right) \\ &= \left( \frac{r^3}{m_e} + 1 + \frac{1}{r} + r^2 \right) \quad \dots (20) \end{aligned}$$

The second term is constant, so it will not be considered. This means that  $\sigma_{ie}^2$  will proportion with the following powers of r:

$$\sigma_{ie}^2 \propto \left( r^3, \frac{1}{r}, r^2 \right) \quad \dots (21)$$

Each term in equation (21) is related to certain parameter that the electrical conductivity depends on, if all these terms are found to work together at

once, then their combination yields  $r^4$  term. Inserting the last term in equation (21) yields:

$$\sigma_{ie}^2 \propto \left( r^3, \frac{1}{r}, r^2, r^4 \right) \quad \dots (22)$$

The terms in equation (22) can be considered as the diagonal of a 4 by 4 matrix then:

$$\sigma_{ie}^2 \propto \begin{pmatrix} r^3 & 0 & 0 & 0 \\ 0 & \frac{1}{r} & 0 & 0 \\ 0 & 0 & r^2 & 0 \\ 0 & 0 & 0 & r^4 \end{pmatrix} \quad \dots (23)$$

Taking the square root of each side in equation (23) yields:

$$\sigma_{ie} \propto \begin{pmatrix} r^{\frac{3}{2}} & 0 & 0 & 0 \\ 0 & \frac{1}{r^{\frac{1}{2}}} & 0 & 0 \\ 0 & 0 & r & 0 \\ 0 & 0 & 0 & r^2 \end{pmatrix} \quad \dots (24)$$

The proportion can be converted to equality by assuming proportionality constants as follows:

$$\sigma_{ie} = \begin{pmatrix} \alpha_1 r^{3/2} & 0 & 0 & 0 \\ 0 & \alpha_2 \frac{1}{r^{1/2}} & 0 & 0 \\ 0 & 0 & \alpha_3 r & 0 \\ 0 & 0 & 0 & \alpha_4 r^2 \end{pmatrix} \quad \dots (25)$$

The matrix in equation (25) can be written as a summation equation as follows:

$$\sigma_{ie} = \alpha_1 r^{3/2} + \alpha_2 \frac{1}{r^{1/2}} + \alpha_3 r + \alpha_4 r^2 + \alpha_0 \quad \dots (26)$$

The fourth factor  $\alpha_4$  represents the case where all the first three factors act together mutually. It can be neglected if the first three factors act independently.  $\alpha_0$  is the intercept parameter.

### 3. Mayadas-Shatzkes model

The effect of grain boundaries on the electrical resistivity of poly crystalline metals is explained theoretically by the Mayadas-Shatzkes (MS) model [16][21]. The model, created in 1970 by A.F. Mayadas and M. Shatzkes, offers a thorough comprehension of how electron scattering at grain boundaries affects a material's total resistivity. The model considers the reflection of the electrons from the grain boundaries which is expressed as R, in addition to scattering mechanisms [29]. The equation derived by the MS model is:

$$\sigma = 3\sigma_o \left( \frac{1}{3} - \frac{1}{2} \frac{\alpha}{d} + \left( \frac{\alpha}{d} \right)^2 - \left( \frac{\alpha}{d} \right)^3 \ln \left( 1 + \frac{d}{\alpha} \right) \right) \quad \dots (27)$$

Where

$$\alpha = l_o \frac{R}{1-R} \quad \dots (28)$$

$l_o$  is the mean free path, and d is the grain size.

#### 4. Andrews model

It is a phenomenological method for explaining how grain boundaries affect poly crystalline metals' electrical resistivity [21][30].

This model shows that the average grain diameter is inversely proportional to the resistivity contribution from grain boundaries, which is phenomenologically known from experiments [31]. In other words, it is directly proportional to conductivity; i.e.  $\sigma \propto d$ , therefore [20]:

$$\sigma = \sigma_a + A'd \dots (29)$$

Where  $\sigma_a$  is the bulk conductivity neglecting the effect of grain boundaries,  $A'$  is a constant. The three models will be applied to experimental data for Cu

and Ni to test their applicability and take advantage in interpreting the variations of electrical conductivity versus grain size.

#### 5. Results and Discussion

In the present work, the three models were applied to the experimental data for the electrical conductivity of Cu and Ni versus grain size from different references [32]–[34].

##### 5.1. For Cu:

Figures 1, 2, and 3 show experimental data on copper's electrical conductivity versus grain size [34] fitted using the time of events model, Mayadas-Shatzkes model, and Andrew model respectively. The fitting parameters are in Table 1.

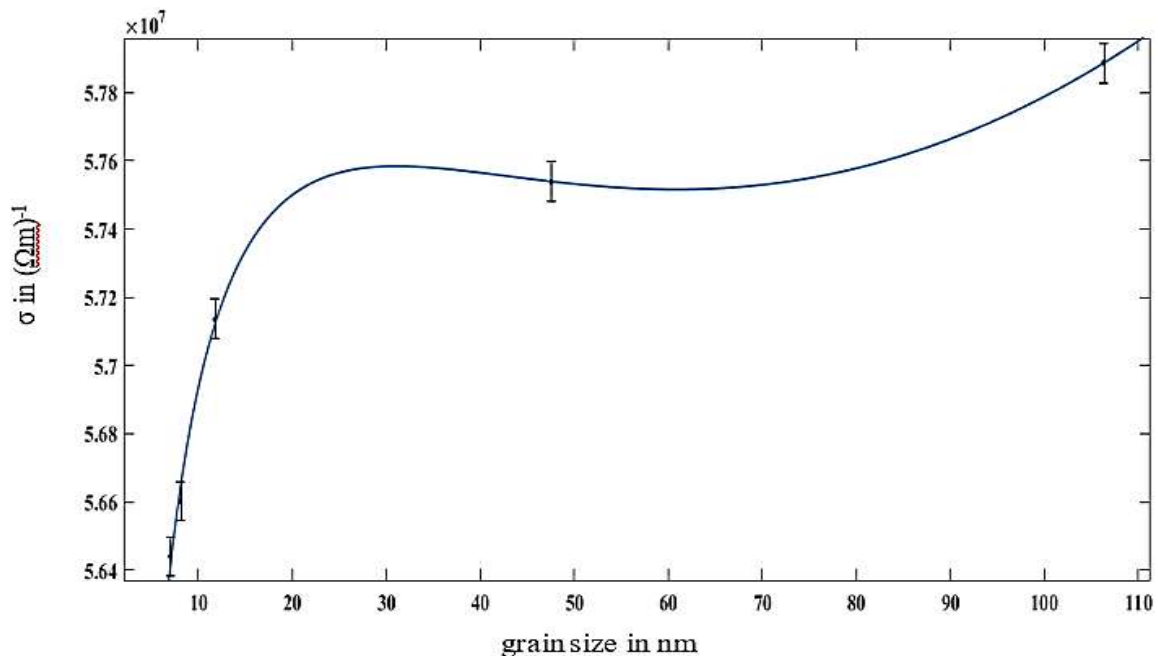


Figure 1. Electrical conductivity versus grains size for copper. The black dots are for experimental data taken from ref. [30]. The blue line is the fitting curve from the time of events model equation (26).

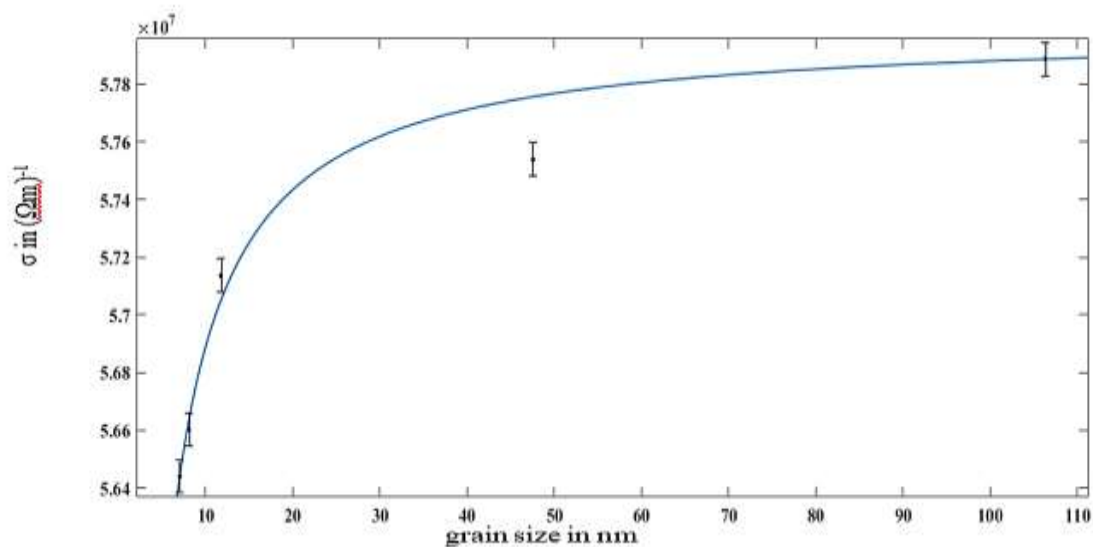


Figure 2. Electrical conductivity versus grains size for copper. The black dots are for experimental data taken from ref. [30]. The blue line is the fitting curve from the Mayadas-Shatzkes model equation (27).

Table 1. Fitting parameters for three models applied to copper data.

Fitting parameters	$\alpha_1$	$\alpha_2$	$\alpha_3$	$\alpha_0$	Adjusted R-square
Time of events model	6273 (-9794, 2.234e+04)	-1.143e+07 (-2.894e+07, 6.077e+06)	-8.545e+04 (-3.033e+05, 1.324e+05)	6.12e+07 (5.374e+07, 6.867e+07)	0.99
Fitting parameters	$\alpha$		$\sigma_0$		
Mayadas-Shatzkes model	0.1303 (0.08606, 0.1746)		5.805e+07 (5.771e+07, 5.839e+07)		0.95
Fitting parameters	$A'$		$\sigma_a$		
Andrews			1.27e+04 (545.1, 2.486e+04)	5.666e+07 (5.602e+07, 5.73e+07)	0.715

where  $\alpha_4$  is neglected because adding it to the fitting process did not make the fitting curve closer to experimental results. The results for copper electrical conductivity show a nonlinear behavior versus grain size in figures from 1 to 3. Figure 3 at relatively large grain sizes shows a slight decrease in conductivity as grain size decreases. However, at a grain size value close to 11 nm, the reduction in conductivity takes steep behavior. Andrews model fits well with the behavior at relatively large grain sizes; however, it cannot predict the steep behavior at extremely tiny grain sizes close to 11 nm. In Figure 2 the Mayadas-Shatzkes model fits well with experimental data at all scales. However, it deviates slightly from experimental results close to 50 nm. The best fitting

result was in Figure 1, where the time of events model showed excellent agreement with the experimental results. This agrees with the adjusted R-square values, where the best result was for the time of events model fitting. The interpretation of the superiority of the time of events model over other models is due to combining the fitting parameter that is active at a large scale which is represented by ( $\alpha_3$ ) in the TE model and  $A'$  in the Andrews model with the active parameters at small scales represented by  $\alpha_2$  and  $\alpha_1$  in TE model.  $\alpha_3$  order in the TE model is the same as the value of  $A'$  in the Andrews model.  $\alpha_1$  is mainly related to a scale close to 50 nm, while  $\alpha_2$  is related to extremely tiny grain sizes below 11 nm.

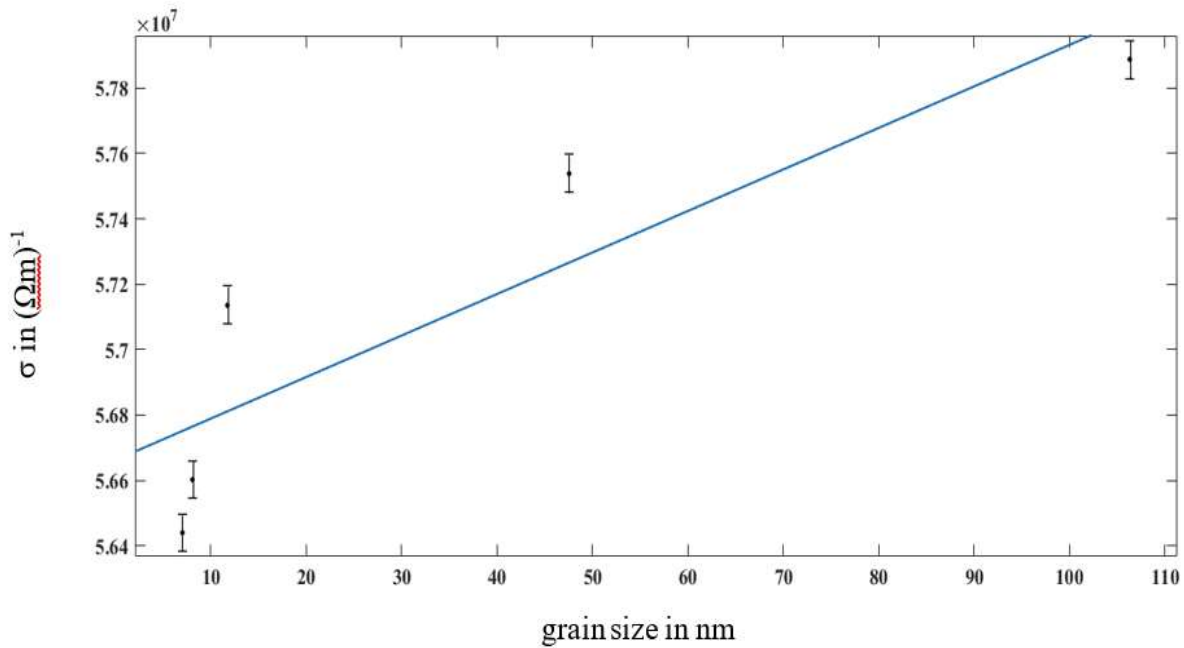


Figure 3. Electrical conductivity versus grain size for copper. The black dots are for experimental data taken from ref. [30]. The blue line is the fitting curve from the Andrew model equation (29).

### 5.2 For Ni:

Figures 4, 5, and 6 show experimental data on copper's electrical conductivity versus grain size [33][35][36] fitted using the time of events model, Mayadas-Shatzkes model, and Andrew model respectively. The fitting parameters are in Table 2.

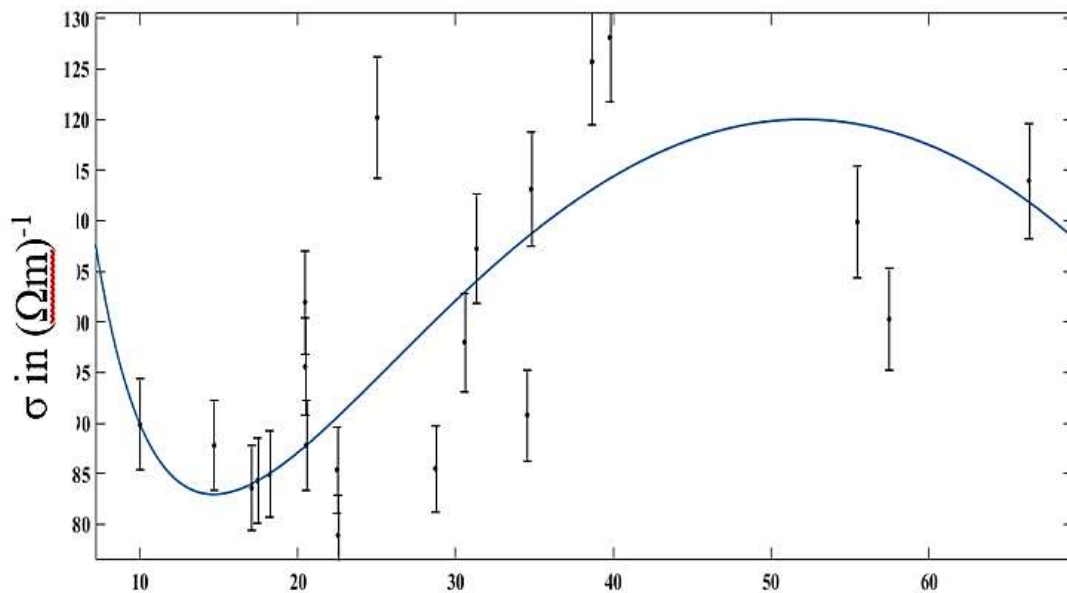


Figure 4. Electrical conductivity versus grain size for nickel. The black dots are for experimental data taken from ref. [31]. The blue line is the fitting curve from the time of events model equation (26).

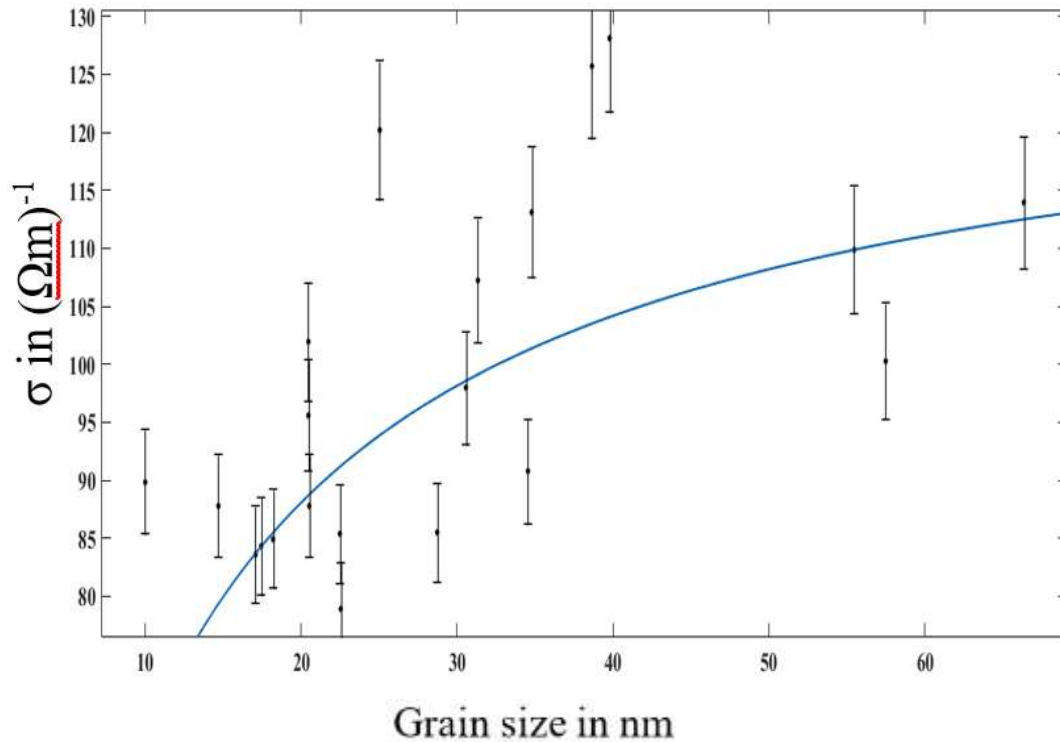


Figure 5. Electrical conductivity versus grain size for nickel. The black dots are for experimental data taken from ref. [31]. The blue line is the fitting curve from the Mayadas-Shatzkes model equation (27).

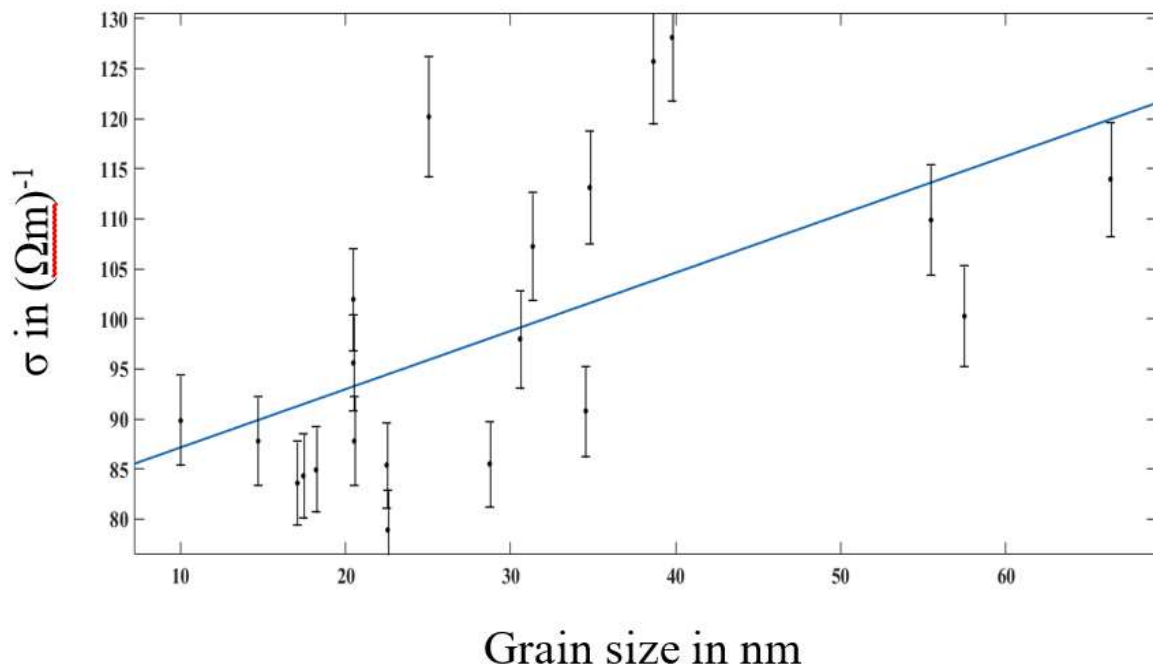


Figure 6. Electrical conductivity versus grains size for nickel. The black dots are for experimental data taken from ref. [31]. The blue line is the fitting curve from the Andrew model equation (29).

Table 2. Fitting parameters for three models applied to nickel data.

Fitting parameters	$\alpha_1$	$\alpha_2$	$\alpha_3$	$\alpha_0$	Adjusted R-square
Time of events model	-1.017 (-2.094, 0.06056)	681.8 (- 189.1, 1553)	11.91 (- 0.2212, 24.04)	-212.6 (-556.5, 131.2)	-
Fitting parameters	$\alpha$		$\sigma_0$		
Mayadas-Shatzkes model	6.474 (1.218, 11.73)		128.6 (102.2, 155.1)		-
Fitting parameters	$A'$		$\sigma_a$		
Andrews model	0.5819 (0.1902, 0.9737)		81.32 (68.31, 94.33)		-

It is noted that the Ni experimental data even if combined from three references [32][33][35], unlike the Cu data is relatively diffused and has high nonlinearities versus grain size. Therefore, the reduced R-square is neglected for Ni data. The relatively wide spread of the experimental data may be due to induced surface effects that lead to increased resistivity specially in thin film samples [14][37]–[40]. Even though the TE model seems to be the closest to experimental data among other models. Andrews model fit is closer to experimental data than Mayadas-Shatzkes model fit. In Ni data also the  $\alpha_3$  parameter in TE model fit is close to the order of  $A'$  in Andrews model. The TE model fit predicted the complex behavior for the Ni data which involves having minima at 15 nm and maxima at 50 nm, where at extremely tiny grain sizes the conductivity slightly decreases with increasing grain size till minima then it increases sharply till 50 nm maxima then it decreases again above this value. Both Andrews and Mayadas-Shatzkes models do not predict this behavior at extremely tiny grain sizes. This complex behavior may be related to the interference between the  $\alpha_1$  and  $\alpha_2$  parameters. In Ni, the difference is only two orders of magnitude between these parameters, while in Cu the difference is four orders of magnitude, this makes interference more difficult between different scales.

## 6. Conclusions

This work presents a new model derived from electrical conductivity versus grain size from the time of events theory. To evaluate the newly derived model, it was applied to experimental data of two metals Cu and Ni due to their importance in electricity transmittance and electrical circuits. In

addition, for comparison, two other models were applied to the experimental data named as Mayadas-Shatzkes model and Andrews model. The TE model showed an excellent agreement with the experimental data of Cu better than both models. However Mayadas-Shatzkes model was also consistent with the experimental data. In Ni data, the data was largely diffused, but the TE model still has good agreement with it which is better than both other models. Additionally, the TE model predicted the complex behavior of Ni data which involves having maxima and minima, while other models did not have such prediction. From comparing the fitting parameter values between Andrews models and TE models, it was observed that one of the parameters of the TE models is close to  $A'$  parameter value, so Andrews model can be considered part of the new model. The reason for the superiority of the TE model is considering the effects that appear at tiny grain sizes through two factors  $\alpha_1$  and  $\alpha_2$ ; where  $\alpha_1$  for extremely tiny grain sizes and  $\alpha_2$  for small grain sizes.

**Acknowledgments:** The authors would like to thank Al-Nahrain University-College of Sciences for supporting publication.

**Funding:** This work is self-funded.

**Conflicts of Interest:** The authors declare no conflict of interest.

## References

- [1] Fadhil, S. A.; Hassan, M. A.; Haseeb, A. S. M. . S. M. A.; Jaafar, H. I.; Al-Ajaj, E. A.; Alrawi, A. H.; Maher, I.; "Manufacturing of porous

- aluminum 2024 alloy samples with impressive compression properties". *Mater. Res. Express*, 6 (7): 076509, 2019.
- [2] Tschöpe, A.; Sommer, E.; Birringer, R.; "Grain size-dependent electrical conductivity of polycrystalline cerium oxide: I. Experiments". *Solid State Ion.*, 139 (3): 255–265, 2001.
- [3] Pietrzak, T. K.; Wasiucione, M.; Garbarczyk, J. E.; "Towards Higher Electric Conductivity and Wider Phase Stability Range via Nanostructured Glass-Ceramics Processing". *Nanomater.*, 11 (5): 1321, 2021.
- [4] Zhao, K.; Hu, Y.; Du, G.; Zhao, Y.; Dong, J.; "Mechanisms of Scaling Effect for Emerging Nanoscale Interconnect Materials". *Nanomater.*, 12 (10): 1760, 2022.
- [5] Menétrey, M.; van Nisselroy, C.; Xu, M.; Hengsteler, J.; Spolenak, R.; Zambelli, T.; "Microstructure-driven electrical conductivity optimization in additively manufactured microscale copper interconnects". *RSC Adv.*, 13 (20): 13575–13585, 2023.
- [6] Hou, J.; Li, X.; Wang, S.; Fan, X.; Li, C.; Wang, Q.; Zhang, Z.; Zhang, Z.; "Quantitative model for grain boundary effects on strength-electrical conductivity relation". *Acta Mater.*, 281: 120390, 2024.
- [7] Wei, L.; Lin-Li, Z.; Xiao-Jing, Z.; "Grain Size Effect on Electrical Conductivity and Giant Magnetoresistance of Bulk Magnetic Polycrystals". *Chinese Phys. Lett.*, 26 (11): 117502, 2009.
- [8] Bishara, H.; Lee, S.; Brink, T.; Ghidelli, M.; Dehm, G.; "Understanding Grain Boundary Electrical Resistivity in Cu: The Effect of Boundary Structure". *ACS Nano*, 15 (10): 16607–16615, 2021.
- [9] Valencia, D.; Wilson, E.; Jiang, Z.; Valencia-Zapata, G. A.; Wang, K.-C.; Klimeck, G.; Povolotskyi, M.; "Grain-Boundary Resistance in Copper Interconnects: From an Atomistic Model to a Neural Network". *Phys. Rev. Appl.*, 9 (4): 44005, 2018.
- [10] Feng, C.; Jiang, L.; "Micromechanics modeling of the electrical conductivity of carbon nanotube (CNT)–polymer nanocomposites". *Compos. Part A Appl. Sci. Manuf.*, 47: 143–149, 2013.
- [11] Tokarska, M.; "A Mixing Model for Describing Electrical Conductivity of a Woven Structure". *Materials (Basel)*, 15 (7): 2512, 2022.
- [12] Govindaraj, G.; "Electron transport in metallic thin films. A comparative study". *Phys. status solidi*, 113 (1): 113–122, 1989.
- [13] Fuchs, K.; "The conductivity of thin metallic films according to the electron theory of metals". *Math. Proc. Cambridge Philos. Soc.*, 34 (1): 100–108, 1938.
- [14] Sondheimer, E. H.; "The mean free path of electrons in metals". *Adv. Phys.*, 1 (1): 1–42, 1952.
- [15] Namba, Y.; "Resistivity and Temperature Coefficient of Thin Metal Films with Rough Surface". *Jpn. J. Appl. Phys.*, 9 (11): 1326, 1970.
- [16] Mayadas, A. F.; Shatzkes, M.; "Electrical-Resistivity Model for Polycrystalline Films: the Case of Arbitrary Reflection at External Surfaces". *Phys. Rev. B*, 1 (4): 1382–1389, 1970.
- [17] Chawla, J. S.; Gstrein, F.; O'Brien, K. P.; Clarke, J. S.; Gall, D.; "Electron scattering at surfaces and grain boundaries in Cu thin films and wires". *Phys. Rev. B*, 84 (23): 235423, 2011.
- [18] Joo, S. H.; Choi, D.; "Numerical evaluation of grain boundary electron scattering in molybdenum thin films: A critical analysis for advanced interconnects". *Vacuum*, 222: 113025, 2024.
- [19] Li, S. L.; Zhang, Q. Y.; Ma, C. Y.; Zhang, C.; Yi, Z.; Pan, L. J.; "Improvement of electrical-resistivity model for polycrystalline films of metals with non-spherical Fermi surface: A case for Os films". *J. Appl. Phys.*, 121 (13): 134503, 2017.
- [20] Andrews, P. V.; "Resistivity due to grain boundaries in pure copper". *Phys. Lett.*, 19 (7): 558–560, 1965.
- [21] Bakonyi, I.; "Accounting for the resistivity contribution of grain boundaries in metals: critical analysis of reported experimental and theoretical data for Ni and Cu". *Eur. Phys. J. Plus*, 136 (4): 410, 2021.
- [22] Fadhil, S. A.; Azeez, J. H.; Hassan, M. A.; "Derivation of a new multiscale model: I. Derivation of the model for the atomic, molecular and nano material scales". *Indian J. Phys.*, 95 (2): 209–217, 2021.
- [23] Fadhil, S. A.; Hassan, M. A.; Azeez, J. H.; Majeed, M. S.; "Derivation of a new multiscale model: II. Deriving a modified Hall-Petch relation from the multiscale model and testing it for nano, micro, and macro materials". In: *3rd International Conference on Sustainable Engineering Techniques (ICSET 2020)*, Baghdad, Iraq, 15 April 2020, IOP Publishing: UK, 2020.
- [24] Fadhil, S. A.; Azeez, J. H.; Whahaeb, A. F.; "Solving the instantaneous response paradox

- of entangled particles using the time of events theory". *Eur. Phys. J. Plus*, 129 (2): 23, 2014.
- [25] Azeez, J. H.; Fadhil, S. A.; Abidin, Z. Z.; "Derivation of a Rotation Curve Model Based on Time of Events Theory and Its Application on Samples of Several Spiral Galaxies". *Sains Malays.*, 53 (11): 3771–3778, 2024.
- [26] Azeez, J. H.; Abidin, Z. Z.; Fadhil, S. A.; Hwang, C.-Y.; "Analyzing Interferometric CO (3-2) Observations of NGC 4039; [Menganalisis Interferometrik CO (3-2) Pemerhatian NGC 4039]". *Sains Malays.*, 51 (4): 1271 – 1282, 2022.
- [27] Fadhil, S. A.; Alrawi, A. H.; Azeez, J. H.; Hassan, M. A.; "A new multiscale model to describe a modified Hall-Petch relation at different scales for nano and micro materials". In: *Advanced Nanotechnology in Engineering and Medical Sciences (Anems) International Conference 2017, Langkawi, Malaysia, 20–21 November 2017*; Mahmoodian, R.; Abdul Razak, B.; AIP Publishing: USA, 2018.
- [28] Azeez, J. H.; Fadhil, S. A.; Abidin, Z. Z.; "Physical properties of the merging galaxy IIZW 096". In: *6th International Conference for Physics and Advance Computation Sciences: ICPAS2024, Baghdad, Iraq, 26 - 27 August 2024*; Obaid, A. J.; Shneishil, A. H.; Mohsen, S. D.; AIP Publishing: USA, 2025.
- [29] Zhang, Q. G.; Zhang, X.; Cao, B. Y.; Fujii, M.; Takahashi, K.; Ikuta, T.; "Influence of grain boundary scattering on the electrical properties of platinum nanofilms". *Appl. Phys. Lett.*, 89 (11): 114102, 2006.
- [30] Güzel, D.; Kaiser, T.; Bishara, H.; Dehm, G.; Menzel, A.; "Revisiting Andrews method and grain boundary resistivity from a computational multiscale perspective". *Mech. Mater.*, 198: 105115, 2024.
- [31] Bishara, H.; Ghidelli, M.; Dehm, G.; "Approaches to Measure the Resistivity of Grain Boundaries in Metals with High Sensitivity and Spatial Resolution: A Case Study Employing Cu". *ACS Appl. Electron. Mater.*, 2 (7): 2049–2056, 2020.
- [32] Madduri, P. V. P.; Kaul, S. N.; "Magnon-induced interband spin-flip scattering contribution to resistivity and magnetoresistance in a nanocrystalline itinerant-electron ferromagnet: Effect of crystallite size". *Phys. Rev. B*, 95 (18): 184402, 2017.
- [33] McCrea, J. L.; Aust, K. T.; Palumbo, G.; Erb, U.; "Electrical Resistivity as a Characterization Tool for Nanocrystalline Metals". *MRS Online Proc. Libr.*, 581 (1): 461–466, 1999.
- [34] Dong, L.; Yang, F.; Yu, T.; Zhang, N.; Zhou, X.; Xie, Z.; Fang, F.; "Contribution of grain boundary to strength and electrical conductivity of annealed copper wires". *J. Mater. Res. Technol.*, 26: 1459–1468, 2023.
- [35] Bakonyi, I.; Isnaini, V. A.; Kolonits, T.; Czigány, Z.; Gubicza, J.; Varga, L. K.; Tóth-Kádár, E.; et al.; "The specific grain-boundary electrical resistivity of Ni". *Philos. Mag.*, 99 (9): 1139–1162, 2019.
- [36] Madduri, P. V. P.; Kaul, S. N.; "Core and surface/interface magnetic anisotropies in nanocrystalline nickel". *J. Alloys Compd.*, 689: 533–541, 2016.
- [37] Sambles, J. R.; "The resistivity of thin metal films—Some critical remarks". *Thin Solid Films*, 106 (4): 321–331, 1983.
- [38] Vancea, J.; Reiss, G.; Hoffmann, H.; "Mean-free-path concept in polycrystalline metals". *Phys. Rev. B*, 35 (12): 6435–6437, 1987.
- [39] Vancea, J.; "Unconventional features of free electrons in polycrystalline metal films". *Int. J. Mod. Phys. B*, 03 (10): 1455–1501, 1989.
- [40] Henriquez, R.; Cancino, S.; Espinosa, A.; Flores, M.; Hoffmann, T.; Kremer, G.; Lisoni, J. G.; Moraga, L.; Morales, R.; Oyarzun, S.; Suarez, M. A.; Zúñiga, A.; Munoz, R. C.; "Electron grain boundary scattering and the resistivity of nanometric metallic structures". *Phys. Rev. B*, 82 (11): 113409, 2010.